Orientation of particles in *Ci* crystal clouds. Part 1. Orientation at gravitational sedimentation

B.V. Kaul[1] and I.V. Samokhvalov[2]

[1] *Institute of Atmospheric Optics, Siberian Branch of the Russian Academy of Sciences, Tomsk*
[2] *Tomsk State University*

Received July 15, 2005

A model of distribution over angles of deviation from the horizontal position of crystal cloud particle maximal diameters in the process of their gravitational sedimentation is proposed. A single-parametric distribution over orientation angles is obtained. The distribution parameter is shown to depend on the particle size and the rate of energy dissipation in the turbulence cells.

Crystal cloud particles are anisotropic. The ratio of their maximal diameters to minimal ones varies from one and a half to some units. At gravitational sedimentation, aerodynamic forces orient particles by their greater diameters crosswise to the direction of the counter air flow.[1,2] At the same time, some forces destructive for the orientation process affect the particles: stochastic fluctuations of the angular momentum due to Brownian rotation, as well as interactions with turbulent micropulsations of the air flow velocity. Estimates show that in the 5–10 μm size range energies of these two disorientation mechanisms are comparable in the order of magnitude. For smaller particles, the thermal motion is a determining factor. For particles of 100 μm size, the energy of interaction with dissipation turbulent cells is three orders of magnitude greater than kT.

Turbulent cells of sizes comparable with particle maximal diameters, effectively destroy the orientation. Large-scale vortices do not affect essentially the particle orientation, but they are responsible for macroscopic transfer, in particular, they prevent from particle size separation over heights in the process of the gravitational sedimentation.[3,4]

The sedimentation orientation is the main orientation mechanism for particles. A possibility of particle orientation by their greater diameters predominantly in some azimuthal direction (presumably, crosswise to the wind velocity), was proved by means of solar column observations[5] and lidar investigations of the backscattering phase matrices.[6] We plan to substantiate this hypothesis in the next paper. Experiments have shown that the azimuth orientation seldom manifests itself strongly, therefore, it can be ignored safely for accuracy in calculations of the scattered radiation angular distribution. Only the angular distribution of deviations of the particle maximal diameters from horizontal position will be discussed below. A uniform angular distribution of the azimuth orientation is supposed.

The material of this paper can be used in designing optical models of crystalline clouds. In particular, in the nearest future, we plan to estimate the correlation between the element m_{44} of the normalized backscattering phase matrix (BSPM) determined at a crystal cloud sensing to zenith or nadir, and parameters of distribution over angles θ of deviation of plate bases or column axes from the horizontal position. It was shown[6,7] that m_{44} does not depend on the azimuth orientation. Its variations for some particular ensemble of particles depend only on variations of the particle distribution function over θ. Since we have in our disposal the instrument (the lidar "Stratosphere") capable of measuring the overall BSPM, we can compare then modeling results with experiment.

Crystal clouds contain particles of various shapes and sizes. According to international classification, there are ten types of particles, and according to a more detailed classification, there are 80 modifications of crystals.[8] Nevertheless, data are available that crystals of columnar and plate-like shapes[9] are prevalent in *Ci* and *Cs* clouds at heights of 6.5–11 km. We will simulate these particles in the orientation model as oblate and elongated ellipsoids of rotation.

The particle size spectrum in crystal clouds of the upper layer lies in the range from several microns to a millimeter. Hence, particle motion regimes are different. Air is a viscous medium for fine particles. Their sedimentation velocity can be estimated by the Stokes formula. The motion character of larger particles is turbulent. We estimate their motion velocity using the known empirical relationship between the sedimentation velocity u and the maximal diameter h

$$u = Ah^{\beta}. \qquad (1)$$

The values of the empirical constants A and β for crystals of different shapes, taken from Ref. 11, are presented in Ref. 12, where the velocity is determined in cm/s, and the maximum size in mm. To turn to the units of SI system, it is necessary to use the constant

$$A^{*} = 10^{3\beta-2}A. \qquad (1')$$

0235-6880/05/11 866-05 $02.00

The comparison of the sedimentation velocities calculated by the Stokes formula and Eq. (1) shows that both formulas provide for approximately equal (from 0.5 to 4 cm/s) velocities for particles with sizes between 5 and 20 μm. As for larger particles, the Stokes formula gives overestimated values as compared to the experimental data. For simplification, we consider Eq. (1) true for all sizes.

The boundary between the regimes of viscous and turbulent motion is near the Reynolds number $\mathrm{Re} \cong 1$. If the particle maximum-size distribution is known, one can determine how the motion of cloud particles is distributed between two aforementioned regimes. Let us take the two-parameter gamma-distribution of the probability density as the initial distribution[12]:

$$f_1(h) = \frac{\mu^{\mu+1}}{\Gamma(\mu+1)h_m}\left(\frac{h}{h_m}\right)^{\mu} \exp\left(-\mu\frac{h}{h_m}\right), \qquad (2)$$

where h is the maximal diameter of particles, $\mu = 4$, $h_m = 4 \cdot 10^{-4}$ m is the distribution mode.

However, a comparison of distribution (2) with later measurements carried out with the improved instrumentation[13,14] leads to the conclusion that this distribution underestimates values for small particles. Therefore, we finally accept the probability distribution

$$f(h) = 0.8f_1(h) + 0.2f_2(h), \qquad (3)$$

where $f_2(h) = \alpha\exp(-\alpha h)$, $\alpha = 10^4$.

The distribution (3) is shown in Fig. 1, for which the following normalizing condition is fulfilled:

$$\int_0^{\infty} f(h)\mathrm{d}h = 1,$$

satisfactorily describing the experimental spectrum presented in Ref. 14.

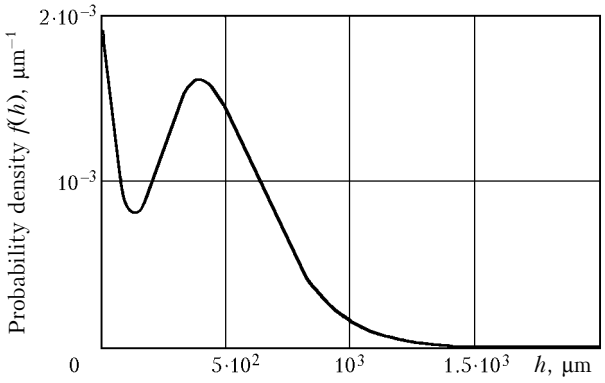

Fig. 1. Distribution of the crystal cloud particles over maximal diameters accepted for estimations of the distribution over the Reynolds numbers.

Using the definition $\mathrm{Re} = uh/\nu$, where ν is the air kinematic viscosity, and the empirical relationship (1), let us pass to distribution over the Reynolds numbers. To do this, we apply the rule for the distribution of random values related by the functional dependence.[15] The distribution over the Reynolds numbers is shown in Fig. 2.

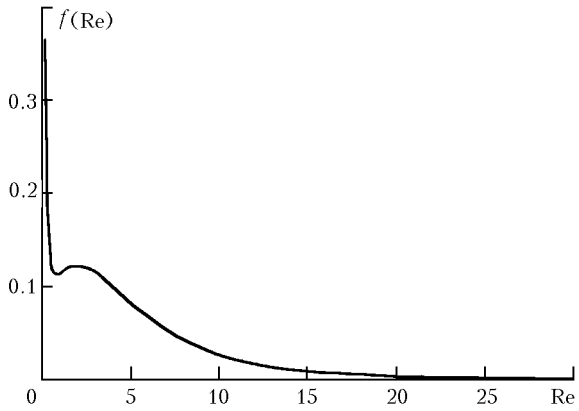

Fig. 2. Distribution over the Reynolds numbers corresponding to the size distribution shown in Fig. 1.

The distribution satisfies the normalizing condition $P(0, \ldots, \infty) = 1$, where P is the total probability. A fraction of particles satisfying the condition $\mathrm{Re} \le 1$ is equal to 0.215. Particle sizes satisfying the same condition correspond to the range $0 < h_m < 200$ μm.

All the aforesaid means that sedimentation of about 80% of cloud particles goes in the regime of generation of turbulent vortices. But the Reynolds numbers do not exceed 10–20, that corresponds to the stationary regime, at which the partial derivative of the flow velocity with respect to time in the coordinate system related to the particle is zero, and the circulation along any contour around the particle is zero. In other words, the vortices are stationary and move together with the particle. All this is related to a stable regime of sedimentation, at which a particle occupies a symmetric position relative to the flow. When deviating from the equilibrium position, the vortex field symmetry is destroyed, and the flow circulation becomes nonzero.

According to the law of conservation of the angular momentum, the particle is affected by the moment of force, the sign of which is opposite to the moment stipulated by the flow velocity circulation. It is essential that $\mathrm{Re} < 40$ for the entire spectrum of particles, hence, the regime of vortex separation, at which particle oscillations are possible, does not occur. The vortices are located near the particle, and the velocity field of the counter airflow can be considered potential, on the average. In this case the module of the moment of forces affecting the ellipsoid of rotation is described by the formula[1,10]

$$M(\theta) = \lambda u^2 \rho V \sin 2\theta / 2, \qquad (4)$$

where θ is the angle between directions of the particle sedimentation velocity u and the small axis of the ellipsoid of rotation; ρ is the air density; V is the ellipsoid volume, λ is the form-factor depending

on the ratio between the minor b and major a semi-axes of the ellipsoid:

$$\lambda = \left\{ e^3 \left[e - \sqrt{1-e^2} \left(\frac{\pi}{2} - \arctan \frac{\sqrt{1-e^2}}{e} \right) \right]^{-1} - 1 \right\}^{-1}, \quad (5)$$

where $e = \sqrt{\left(a^2 - b^2\right)/a^2}$ is the eccentricity.

The volumes of spheroid and elongated ellipsoid can be expressed through dimensions of big semi-axes and the eccentricity by the following formulas:

$$V_s = \frac{4}{3}\pi a^3 \sqrt{1-e^2}, \quad V_e = \frac{4}{3}\pi a^3 (1-e^2). \quad (6)$$

Substitute $a = h/2$ into Eq. (6), where h stand for maximal diameters of particles, and determine the sedimentation velocity from Eq. (1) taking into account Eq. (1′).

Then we obtain for the orienting moment:

$$M_s(\theta) = \frac{1}{12}\pi \Lambda_s \rho A^2 \cdot 10^{(6\beta-4)} h^{3+2\beta} \sin 2\theta \quad (7)$$

for plate-like particles, and

$$M_e(\theta) = \frac{1}{12}\pi \Lambda_e \rho A^2 \cdot 10^{(6\beta-4)} h^{3+2\beta} \sin 2\theta \quad (8)$$

for columnar ones,

where $\Lambda_s = \lambda\sqrt{1-e^2}$ and $\Lambda_e = \lambda(1-e^2)$ are the generalized form-factors.

The energy needed for realization of the ensemble of N particles with the size distribution $f(h)$ deviated from the equilibrium position through the angle θ, is

$$U(\theta) = N \int_0^{\theta} \int_0^{\infty} M(\theta, h) f(h) \mathrm{d}h \mathrm{d}\theta. \quad (9)$$

It depends only on the generalized coordinate θ and can be considered as the potential energy of the particle ensemble. A decrease of energy in the equilibrium state is compensated for at the cost of interaction of particles with turbulent micropulsation cells, the kinetic energy of which is proportional to the air mass in the cell multiplied by the mean square of the velocity pulsations $\left\langle u_t^2 \right\rangle$.

Let us determine the scales of length and velocity in the dissipation interval[16]:

$$l = \left(\frac{\nu^3}{\varepsilon} \right)^{1/4}, \quad u_t = (\varepsilon\nu)^{1/4}, \quad (10)$$

where ε is the energy dissipation rate. Take in estimation that $T = 250$ K and $\nu = 3 \cdot 10^{-5}$ m^2/s correspond to a height of 10 km. The dissipation rate strongly depends on the turbulent state of the atmosphere. In average, for tropopause $\varepsilon = 4$–$5 \cdot 10^{-4}$ m^2/s^3 (~ 4–5 cm^2/s^3), but in clouds the values can be tens and hundreds times higher.[17] Note that for the above ε and ν $u_t \cong 3.5 \cdot 10^{-2}$ m/s, and $l \cong 2.5$ mm.

The cell of l diameter has, on the average, the energy

$$w = \frac{1}{6}\pi l^3 \rho \left\langle u_t^2 \right\rangle. \quad (11)$$

Determine the cell energy as the function of the mean dissipation rate, using Eqs. (10) and (11)

$$w(\varepsilon) = \frac{1}{6}\pi\rho\nu^{11/4}\varepsilon^{-1/4}. \quad (12)$$

We take the efficiency of energy transfer from the turbulent cell to a particle equal to the ratio of their volumes

$$p(\varepsilon, h) = h^3 (\nu^3/\varepsilon)^{-3/4}. \quad (13)$$

The kinetic energy received by the particle at collision with the cell is

$$W(h, \varepsilon) = p(h, \varepsilon) w(\varepsilon). \quad (14)$$

Now we find the distribution over the orientation angle from the condition of the balance between the potential energy of particles and the kinetic energy of the turbulent pulsations

$$\mathrm{d}U(\theta, h) + \mathrm{d}E(\varepsilon, h) = 0. \quad (15)$$

First suppose that the ensemble consists of n particles of the same size $\bar{h}$. Then Eq. (15) can be rewritten as

$$nM(\theta, \bar{h})\mathrm{d}\theta = -W(\bar{h}, \varepsilon)\mathrm{d}n. \quad (16)$$

Integration of this equation results in

$$n(\theta) = C \exp(\chi \cos 2\theta), \quad (17)$$

where, taking into account Eqs. (7), (8), (12)–(14),

$$\chi(\bar{h}, \varepsilon) = \Lambda_{s,e} 10^{(6\beta-4)} A^2 \bar{h}^{2\beta} / 4\sqrt{\nu\varepsilon}. \quad (18)$$

The dependence of χ on large diameters of particles h at five values of the dissipation rate ε is shown in Fig. 3. The χ values for some particle sizes are shown in Table 1.

The distribution shape for three χ values is shown in Fig. 4. At $\chi \to 0$ the distribution is transformed to the uniform one with the probability density $1/\pi$. The values of the square root of the variance σ are shown in Table 2, which give an estimate of the flatter magnitude at given values of χ.

According to Eq. (18), χ can be considered as the function of the greater diameter h at the *a priori* set ε. Since h varies in a wide range, the distribution over the angle θ can not be represented by one function of the form (17) for the overall particle ensemble. To construct the model of distribution over orientation angles suitable for simulation of elements of the scattering phase matrix, we proceed as follows.

Table 1. Dependence of the distribution parameter χ on the maximum diameter of particles *h* at five values of the energy dissipation rate ε. Upper values are for plate-like particles, lower are for columns

ε, m^2/s^3	*h*, μm										
	5	10	20	30	50	100	200	300	400	500	750
10^{-4}	0.20	0.71	1.61	2.97	6.38	18.0	51.0	93.7	144	202	372
	0.04	0.14	0.50	1.06	2.71	19.9	34.7	73.2	124	187	395
$5 \cdot 10^{-4}$	0.09	0.25	0.72	1.33	2.85	8.07	22.8	41.9	64.5	90.2	166
	0.02	0.06	0.22	0.47	2.21	4.34	15.5	32.7	55.6	83.8	176
$5 \cdot 10^{-3}$	0.03	0.08	0.23	0.42	0.90	2.55	7.22	13.3	20.4	28.5	52.4
	0.01	0.02	0.07	0.15	0.38	1.37	4.91	10.4	17.6	26.5	55.9
10^{-2}	0.01	0.03	0.07	0.13	0.28	0.81	2.28	4.19	6.45	9.02	16.6
	—	0.01	0.02	0.05	0.12	0.43	1.55	3.27	5.56	8.38	17.7
$5 \cdot 10^{-1}$	—	0.01	0.02	0.04	0.09	0.25	0.72	1.33	2.04	2.85	5.24
	—	—	—	0.01	0.04	0.14	0.49	1.04	1.77	2.65	5.59

Table 2. Rms deviations from the horizontal position

χ	1	3	5	10	30	50	100	200	300	500
$(\sqrt{\sigma})^\circ$	36.3	18.9	13.7	9.3	5.3	4.1	2.9	2.0	1.6	1.3

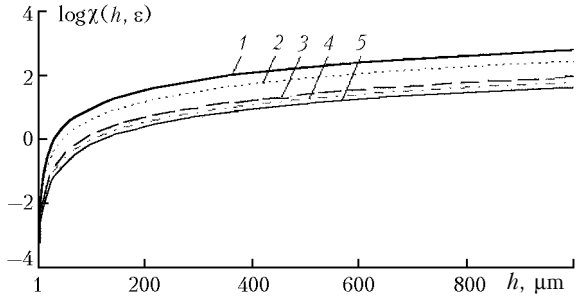

Fig. 3. Dependence of the distribution parameter $\chi(h, \varepsilon)$ over the orientation angles (17) on the diameter of plate-like particles h at the following values of energy dissipation rate ε, m^2/s^3: 10^{-4} (*1*); $5 \cdot 10^{-4}$ (*2*); 10^{-3} (*3*); 10^{-2} (*4*); $5 \cdot 10^{-1}$ (*5*).

Select some sub-ensemble of particles in the size range $[h_{i-1}, h_i]$, within which we can make use of the mean size $h_i = \bar{h}_i$. Statistical weight of such a sub-ensemble and the number density of particles are, respectively,

$$g_i = \int_{h_{i-1}}^{h_i} f(h)\mathrm{d}h, \quad n_i = g_i N, \quad \bar{h}_i = \int_{h_{i-1}}^{h_i} hf(h)\mathrm{d}h, \qquad (19)$$

where N is the total number density of particles. The normalizing constant is determined from the condition

$$\int_{-\pi/2}^{\pi/2} n_i(\theta)\mathrm{d}\theta = g_i N;$$

$$C_i = g_i N \left\{ \int_{-\pi/2}^{\pi/2} \left[\exp(\chi_i(\bar{h}_i, \varepsilon)\cos 2\theta) \right] \mathrm{d}\theta \right\}^{-1} =$$

$$= g_i N / \pi I_0(\chi_i), \qquad (20)$$

where $I_0(\chi)$ is the modified Bessel function of zero order.

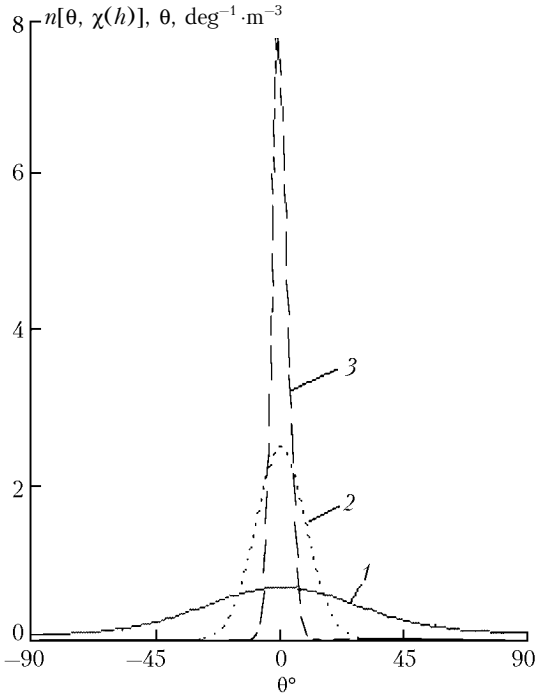

Fig. 4. Distribution function over the deviation angle θ of maximal particle diameters from horizontal position at the following values of the distribution parameter $\chi(h, \varepsilon)$: χ = 1 (*1*); 10 (*2*); 100 (*3*).

The model of distribution over the angle θ for the overall ensemble is represented by a set of functions of the form

$$n_i(\theta) = C_i \left[\exp(\chi(\bar{h}_i, \varepsilon)\cos 2\theta) \right]. \qquad (21)$$

Note that any size-distribution function, for which the condition $\mathrm{Re} = A^* h^\beta \nu \le 40$ is fulfilled, can be taken as the function $f(h)$ in definitions (19).

It follows from the aforesaid that the interaction of the falling crystal particles with the collective motion of molecules in dissipation cells is the determining factor in distribution over orientation

angles. If to admit that disorientation occurs only due to the thermal motion of molecules, our estimates show the following. The particles smaller than 5 μm are completely disoriented. Orientation of larger particles quickly increases so that the rms deviation for 10 μm particles is about 7°, and 20 μm particles are, in practice, strictly oriented. However, this contradicts to the experimental data obtained at the Institute of Experimental Meteorology.[18]

Observations with a TV-camera have shown that the horizontal orientation of ice columns of $d = 36$ μm and $h = 54$ μm is only one order of magnitude higher than the vertical orientation. This corresponds sooner to the lower value (2.71) in the fifth column of the first row in Table 1.

In closing, we would like to remark upon conclusions inferred in Ref. 3 about the turbulence effect on particle orientation in a cumulus cloud. The qualitative analysis based on comparison of linear scales of the orientation distance (the product of the particle sedimentation velocity into the orientation time), linear scale of the dissipation cell (10), and the Taylor microscale has led the authors to some, in our opinion, vigorous conclusion about insignificant effect of turbulence on the particle orientation. The lower row of Table 1 is calculated for the turbulence parameters used by authors of the cited paper. They took a particle size of 500 μm. As is seen in Table 1, a noticeable orientation is still observed for particles of such a size, but it is far from that, which would occur in the absence of turbulence.

The estimate[3] of the probability of particle collision with a dissipation cell based on comparison of the cell volumes of the scale (10) and the Taylor cells seems to be incorrect. Obviously, they have ignored the fact that there is a continuous energy spectrum between two aforementioned scales, and the process of energy dissipation is most intensive in the range $0.1 < kl < 1$, where k is the wave number,[16] that corresponds to the range $6l - 60l$ of the cell linear sizes. Taking into account of only this fact increases the estimate of probability by the technique developed by the authors, by two orders of magnitude. Actually, the probability of the event that a particle will be subjected to impact of some dissipation cell of one or another size, is quite high.

Acknowledgments

This work was supported in part by Russian Foundation for Basic Research (Grant No. 04–05–64495) and Federal Agency of Science and Innovations of the Ministry of Education and Science of Russian Federation (state contract No. RI 26/071).

References

1. N.A. Fuchs, *Aerosol Mechanics* (Academy of Sciences of USSR, Moscow, 1955), 450 pp.
2. Yu.D. Kopytin, A.A. Chursin, G.A. Chursina, and S.A. Shishigin, Atmos. Oceanic Opt. **3**, No. 10, 998–1002 (1990).
3. H.-R. Cho, J.V. Iribarne, and W.G. Richards, J. Atmos. Sci. **38**, No. 5, 1111–1114 (1981).
4. G.G. Matvienko, G.O. Zadde, E.S. Ferdinandov, I.N. Kolev, and R.P. Avramova, *Correlation Techniques for Laser-Radar Measurements of Wind Velocity* (Nauka, Novosibirsk, 1985), 221 pp.
5. K. Langgenhager, Zeitschrift für Meteorol. **27**, No. 3, 179–183 (1977).
6. B.V. Kaul, S.N. Volkov, and I.V. Samokhvalov, Atmos. Oceanic Opt. **16**, No. 4, 325–332 (2003).
7. B.V. Kaul, Atmos. Oceanic Opt. **13**, No. 10, 829–833 (2000).
8. G. Magono and C.W. Lee, J. Fac. Sci. Hokkaido Univ., Ser. 7 (Geophys.), No. 2, 321–335 (1966).
9. A.J. Heymsfield, J. Atmos. Sci. **32**, No. 4, 799–808 (1975).
10. L.M. Minl-Tompson, *Theoretical Hydrodynamics* [Russian translation] (Mir, Moscow, 1964), 497 pp.
11. J. Zikmunda and G. Vali, *Observations of Fall Patterns for Natural Ice Crystals,* College of Engineering. Univ. Wyoming. Rep. N AR103 (1972), 49 pp.
12. O.A. Volkovitskii, L.N. Pavlova, and A.G. Petrushin, *Optical Properties of Crystal Clouds* (Gidrometeoizdat, Leningrad, 1984), 198 pp.
13. W.P. Arnott and J. Hallet, in: *Cirrus: OSA Technical Digest* (Washington DC, 1998), pp. 86–88.
14. R.P. Lawson, in: *Cirrus: OSA Technical Digest* (Washington DC, 1998), pp. 113–115.
15. G.A. Korn and T.M. Korn, *Mathematical Handbook for Scientists and Engineers* (McGraw-Hill, New York, 1961).
16. A.J. Reynolds, *Turbulent Flows in Engineering Applications* (Energia, Moscow, 1979), 405 pp.
17. *Atmosphere,* Handbook (Gidrometeoizdat, Leningrad, 1991), 509 pp.
18. V.V. Kuznetsov, N.K. Nikiforova, L.N. Pavlova, et al., Tr. Ins. Exp. Meteorol., Issue 7 (112), 101–106 (1983).